Molecular Psychiatry (2015), 1–11

www.nature.com/mp

ORIGINAL ARTICLE

Optogenetic activation of intracellular adenosine A_{2A} receptor signaling in the hippocampus is sufficient to trigger CREB phosphorylation and impair memory

P Li[1,2], D Rial[3], PM Canas[3], J-H Yoo[1], W Li[1,2], X Zhou[4], Y Wang[1], GJP van Westen[5], M-P Payen[1], E Augusto[1,3,6], N Gonçalves[3], AR Tomé[3], Z Li[4], Z Wu[4], X Hou[1], Y Zhou[2], Ad PIJzerman[5], ES Boyden[7], RA Cunha[3,6], J Qu[4] and J-F Chen[1,4]

Human and animal studies have converged to suggest that caffeine consumption prevents memory deficits in aging and Alzheimer's disease through the antagonism of adenosine A_{2A} receptors (A_{2A}Rs). To test if A_{2A}R activation in the hippocampus is actually sufficient to impair memory function and to begin elucidating the intracellular pathways operated by A_{2A}R, we have developed a chimeric rhodopsin-A_{2A}R protein (*optoA_{2A}R*), which retains the extracellular and transmembrane domains of rhodopsin (conferring light responsiveness and eliminating adenosine-binding pockets) fused to the intracellular loop of A_{2A}R to confer specific A_{2A}R signaling. The specificity of the *optoA_{2A}R* signaling was confirmed by light-induced selective enhancement of cAMP and phospho-mitogen-activated protein kinase (p-MAPK) (but not cGMP) levels in human embryonic kidney 293 (HEK293) cells, which was abolished by a point mutation at the C terminal of A_{2A}R. Supporting its physiological relevance, *optoA_{2A}R* activation and the A_{2A}R agonist CGS21680 produced similar activation of cAMP and p-MAPK signaling in HEK293 cells, of p-MAPK in the nucleus accumbens and of c-Fos/phosphorylated-CREB (p-CREB) in the hippocampus, and similarly enhanced long-term potentiation in the hippocampus. Remarkably, *optoA_{2A}R* activation triggered a preferential p-CREB signaling in the hippocampus and impaired spatial memory performance, while *optoA_{2A}R* activation in the nucleus accumbens triggered MAPK signaling and modulated locomotor activity. This shows that the recruitment of intracellular A_{2A}R signaling in the hippocampus is sufficient to trigger memory dysfunction. Furthermore, the demonstration that the biased A_{2A}R signaling and functions depend on intracellular A_{2A}R loops prompts the possibility of targeting the intracellular A_{2A}R-interacting partners to selectively control different neuropsychiatric behaviors.

Molecular Psychiatry advance online publication, 17 February 2015; doi:10.1038/mp.2014.182

INTRODUCTION

Recently, six longitudinal prospective studies have established an inverse relationship between caffeine consumption and the risk of developing cognitive impairments in aging and Alzheimer's disease (AD).[1–7] This is in notable agreement with animal studies, which showed that caffeine prevents memory impairments in models of AD[8–10] and sporadic dementia[11] and in other conditions affecting memory performance;[12,13] this seems to involve the antagonism of G-protein-coupled adenosine A_{2A} receptors (A_{2A}Rs), as their selective pharmacological or genetic blockade mimic caffeine's effects.[8,12,14,15] The convergence of human epidemiological and animal evidence led us to propose that A_{2A}Rs represent a novel therapeutic target to improve cognitive impairments in neurodegenerative disorders. The validity of this target is supported by our finding that A_{2A}R inactivation not only enhances working memory,[16,17] reversal learning,[17] goal-directed behavior[18] and Pavlovian fear conditioning[19] in normal animals but also reverse memory impairments in animal models of Parkinson's disease,[20] aging[15] and AD.[8,9,14] Notably, pathological brain conditions associated with memory impairment (such as AD, stress or inflammation) are associated with increased extracellular levels of adenosine[21] and an upregulation and aberrant signaling of A_{2A}R.[22,23] This prompts the hypothesis that the 'abnormal' activation of A_{2A}R in a particular brain region (such as the hippocampus) is sufficient to trigger memory impairment. This critical question has yet to be answered because of the inability to control forebrain A_{2A}R signaling in freely behaving animals with a temporal resolution relevant to behavior.

Another major unsolved question is the mechanisms operated by brain A_{2A}R to control memory function. In fact, A_{2A}R signaling is different in different cellular elements with distinct functions under various physiological vs pathological conditions.[22,24,25] For example, striatal and extrastriatal A_{2A}R exert opposite control of DARPP-32 phosphorylation,[26] c-Fos expression,[26] psychomotor activity[26,27] and cognitive function.[19] Receptor–receptor heterodimerization has been postulated to contribute to the complexity of A_{2A}R signaling.[28] Additionally, recent biochemical studies identified six G-protein-interacting partners (GIP) linked to the intracellular C-terminal tail of A_{2A}R,[29,30] which raises the

[1]Department of Neurology and Pharmacology, Boston University School of Medicine, Boston, MA, USA; [2]Molecular Biology Center, State Key Laboratory of Trauma, Burn, and Combined Injury, Research Institute of Surgery and Daping Hospital, Third Military Medical University, Chongqing, China; [3]CNC – Center for Neurosciences and Cell Biology, University of Coimbra, Coimbra, Portugal; [4]School of Optometry and Ophthalmology and Eye Hospital, Wenzhou Medical College Wenzhou, Zhejiang, China; [5]Leiden Academic Centre for Drug Research, Leiden University, Leiden, The Netherlands; [6]Faculty of Medicine, University of Coimbra, Coimbra, Portugal and [7]MIT Media Lab, Departments of Biological Engineering and Brain and Cognitive Sciences, MIT McGovern Institute, MIT, Cambridge, MA, USA. Correspondence: Dr J-F Chen, Department of Neurology and Pharmacology, Boston University School of Medicine, Boston, 02118 MA, USA.
E-mail: chenjf@bu.edu
Received 5 March 2014; revised 28 October 2014; accepted 12 November 2014

intriguing possibility that the interaction of $A_{2A}R$ intracellular domains with different GIPs may dictate the biased $A_{2A}R$ signaling in different cells. However, the inability to control intracellular GPCR signaling *in vivo* in a precise spatiotemporal manner has prevented translation of *in vitro* profiles of $A_{2A}R$ signaling into behavior in intact animals.

To determine if the abnormal activation of $A_{2A}R$ signaling in the hippocampus is sufficient to impair memory function in freely behaving animals and to begin elucidating the nature of the biased $A_{2A}R$ signaling in different brain regions, we have developed a chimeric rhodopsin-$A_{2A}R$ protein (*optoA$_{2A}$R*): this merges the extracellular and transmembrane domains of rhodopsin conferring light responsiveness and the intracellular domains of $A_{2A}R$ conferring specific $A_{2A}R$ signaling, to investigate the biased $A_{2A}R$ signaling in defined cell populations of freely behaving animals in a temporally precise and reversible manner.[31] Furthermore, the selective retention of only the intracellular domains of $A_{2A}R$ in *optoA$_{2A}$R* chimera permits a critical evaluation of its particular role controlling the biased $A_{2A}R$ signaling. After validating the specificity and physiological relevance of light-induced *optoA$_{2A}$R* recruitment of $A_{2A}R$ signaling in human embryonic kidney 293 (HEK293) cells, mouse brain slices and in freely behaving animals, we exploited its unique temporal and spatial resolution to provide direct evidence that the activation of intracellular $A_{2A}R$ signaling selectively in the hippocampus is sufficient to recruit cAMP and phosphorylated-CREB (p-CREB), and alter synaptic plasticity and memory performance. Our findings also provide a direct demonstration that the intracellular control of the biased $A_{2A}R$ signaling in striatal and hippocampal neurons triggers distinct signaling and behavioral responses.

MATERIALS AND METHODS

Design and construction of the *optoA$_{2A}$R* vector

We have developed a chimeric protein *optoA$_{2A}$R* by replacing the intracellular domain of rhodopsin with those of the $A_{2A}R$ (Figure 1a). We first aligned the conserved residues of the sequence of the $A_{2A}R$ (NCBI accession no. NM_000675.4) with the bovine rhodopsin (NCBI accession no. P02699), and identified the intracellular loops 1, 2 and 3 of $A_{2A}R$ to be exchanged with the intracellular loops of rhodopsin (Figure 1a). Then, we constructed a fusion gene encoding a chimera (*optoA$_{2A}$R*) by replacing the intracellular loops 1, 2 and 3 and the C terminal of rhodopsin with those of $A_{2A}R$ and by adding the C-terminal sequence of bovine rhodopsin (TETSQVAPA) to the C terminal of *optoA$_{2A}$R*. Lastly, codon-optimized sequences of *optoA$_{2A}$R* were fused to the N terminus of mCherry (with its start codon deleted) with a linker (5′-GCGGCCGCC-3′) for fluorescence detection of *optoA$_{2A}$R* in cells and tissues. The *optoA$_{2A}$R* construct was cloned into a pcDNA3.1 vector at the *Eco*RI–*Xho*I sites.

Transfection and detection of *optoA$_{2A}$R* in HEK293 cells

HEK293FT cells were transfected using Lipofectamine 2000 (Invitrogen, Carlsbad, CA, USA) according to the Invitrogen protocols, and the red fluorescence of mCherry was detected 48 h after transfection. To study *optoA$_{2A}$R* signaling, all-*trans*-retinal (25 μM) were added and incubated at 37 °C with 5% atmospheric CO_2 for 60 min. The cells were then illuminated with 500 nm light at 3 mW mm^{-2} using a high-intensity fiber-coupled light source (OSL1-EC; Thorlabs, Newton, NJ, USA). The cells were then fixed with 4% paraformaldehyde for 10 min and permeabilized with 0.1% Triton X-100 in phosphate-buffered saline (PBS). Cells were blocked with 10% normal goat serum and incubated with anti-$A_{2A}R$ (Santa Cruz, Dallas, TX, USA; sc-70321; 1:200) or anti-*P*-MAPK antibodies (Cell Signalling, Danvers, MA, USA; 1:200) overnight at 4 °C. After extensive washes with phosphate buffer saline, cells were incubated with Alexa Fluor 488-conjugated secondary antibodies (Molecular Probes, Eugene, OR, USA) for 60 min at room temperature.

Assessment of *optoA$_{2A}$R* signaling in HEK cells

For bioluminescent assay, HEK293 cells, kept in 96-well plates, were illuminated (500 nm, 3 mW mm^{-2}) for 60 sec. The cells were then lysed 30 min after cessation of light illumination to analyze cAMP using cAMP-Glo™ assay (Promega, Madison, WI, USA), cGMP by HTRF cGMP assay and IP1 by HTRF IP1 assay kit (CisBio, Sunnyvale, CA, USA.). For western blot, cells were isolated at 10 min after light illumination, using a PARIS Kit (Invitrogen). Equal amounts of protein were separated by sodium dodecyl sulfate-polyacrylamide gel electrophoresis (10% gels) and transferred onto an Immobilon-P PVDF membrane (Millipore, Billerica, MA, USA). The membranes were blocked for 1 h in Tris-buffered saline with Tween-20 (TBS-T, pH 7.6) containing 5% non-fat dry milk powder and thereafter incubated overnight at 4 °C with antibodies against mitogen-activated protein kinase (MAPK, Danvers, MA, USA) (Cell Signalling, 1:500), phospho-MAPK (p-MAPK) (Cell Signalling; 1:500) or $A_{2A}R$ (Santa Cruz; 1:1000). The membranes were then probed with different conjugated secondary antibody (Vector Laboratories, Burlingame, CA, USA; 1:3000) at room temperature for 90 min, followed by washing in TBS-T.

Viral production

Recombinant AAV vectors were constructed with a transgene cassette encoding CaMKIIα promoter by cloning the *optoA$_{2A}$R*-mCherry into pAAV-CaMKIIα-eNpHR 3.0-EYFP (Addgene, Cambridge, MA, USA) using *Bam*HI/*Hind*III assisted by GeneScript (Piscataway, NJ, USA). Viral particles were packaged and purified by vector core at the University of North Carolina (Chapel Hill, NC, USA) for serotype 5, and titers were 1.5×10^{12} particles per ml. The AAV5-CaMKIIα-mCherry was purchased from the University of North Carolina at Chapel Hill as 'control' virus with a titer of 2.0×10^{12} particles per ml.

Animals

All procedures were in accordance with the National Institutes of Health Guide and with EU guidelines for the care and use of laboratory animals and approved by the IACUC at the Boston University School of Medicine (Boston, MA, USA; AN no.14684) and by University of Coimbra (Coimbta, Portugal; ORBEA-78-2013 ethical approval). C57BL/6 mice at 11–13 weeks old (weighing 24–28 g) were used in the study. The $A_{2A}R$ knockout mice on a C57BL/6 background were described previously.[32]

Animal surgery: CNS injection and cannulas implantation

Animals were anesthetized with Avertin (10 ml kg^{-1} intraperitoneally). Under a stereotactic frame, a midline scalp incision was made and a ~1 mm diameter craniotomy was drilled to the right nucleus accumbens (NAc; AP, +1.1 mm; ML, ± 1.4 mm; DV, +4.5 mm) or the hippocampus (AP, − 2.2 mm; ML, ± 1.5 mm; DV, +2.3 mm). To express *optoA$_{2A}$R* in neurons of the NAc or hippocampus, we injected 1.0 μl of AAV5-CaMKIIα-*optoA$_{2A}$R*-mCherry virus or 0.75 μl of AAV5-CaMKIIa-mCherry ('control') virus at 0.1 μl $^{-1}$. To activate the endogenous $A_{2A}R$ in the NAc and hippocampus, we injected 2.0 μl of the $A_{2A}R$ agonist CGS21680 (0.5 μg μl^{-1}) at 0.1 μl min^{-1} using an automated syringe pump using a beveled 33-gauge needle. Following the injection, the needle was left for 5 min to allow the drug diffusion. The mice were killed after 15 min and 1 h after injection and processed for immunohistochemistry. We also bilaterally implanted guide cannulae (Plastics One, Roanoke, VA, USA) on the skull through the craniotomy, to bilaterally target the two hippocampi or the two NAc, which were secured using dental cement (Lang Dental, Wheeling, IL, USA). Animals were allowed to recover for at least 2 weeks before the experiment.

Electrophysiological recordings of synaptic plasticity in hippocampal slices

The experiments were carried out as described previously.[33] The hippocampus was dissected in an ice-cold Krebs solution and slices (400 μm) were prepared with a McIllwain chopper. Individual slices were transferred to a submersion recording chamber (1 ml capacity) and continuously superfused at a rate of 3 ml min^{-1} with gassed Krebs solution (composition in mM: NaCl 124, KCl 3, NaH_2PO_4 1.25, glucose 10, $NaHCO_3$ 26, $MgSO_4$ 1, $CaCl_2$) kept at 30.5 °C. A bipolar concentric electrode was placed onto the Schaffer collateral/commissural pathway fibers and stimulated every 20 s with rectangular pulses of 0.1 ms with a Grass S44 pulse generator (PSIU6; Grass, West Warwick, RI, USA). The orthodromically evoked field excitatory postsynaptic potentials were recorded through an extracellular glass microelectrode (filled with 4 M NaCl; resistance: 2–4 MΩ) placed in the *stratum radiatum* of the CA1 area. The high-frequency stimulation (HFS) protocol used to induce long-term potentiation (LTP) consisted of a 100 Hz train during 1 s. Light stimuli consisted of

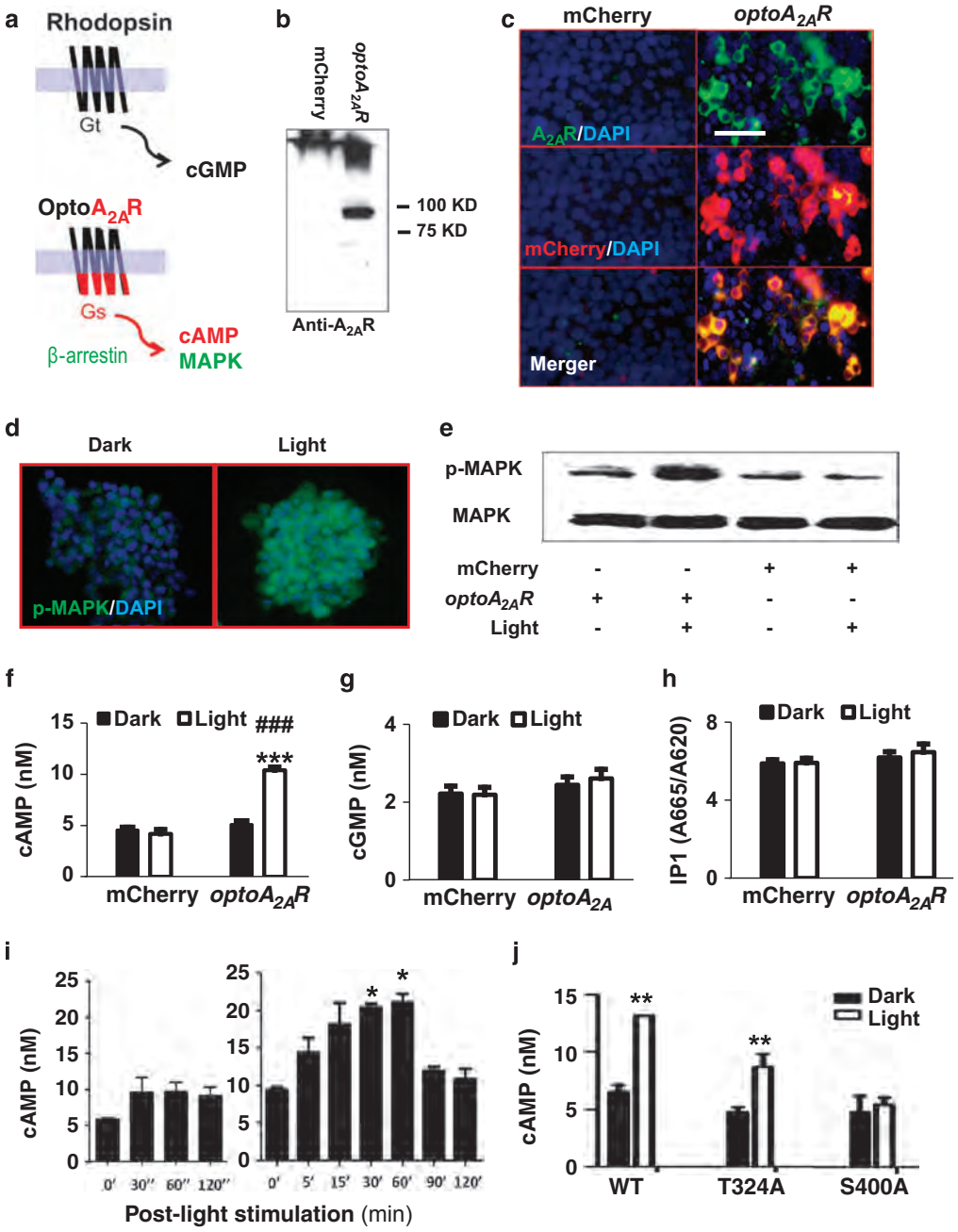

Figure 1. Characterization of *optoA$_{2A}$R* signaling in human embryonic kidney 293 (HEK293) cells. Design (**a**) of *optoA$_{2A}$R* and its expression (b and **c**) in HEK293 cells 24 h after transfection. (**b**) Western blot analysis of *optoA$_{2A}$R* with a molecular weight of 75–100 kDa. (**c**) Colocalization of A_{2A}R immunostaining (green) with mCherry-expressing (red) in *optoA$_{2A}$R*–positive cells. (**d** and **e**) Light induction of phospho-mitogen-activated protein kinase (p-MAPK) in *optoA$_{2A}$R*-expressing cells. (**d**) p-MAPK immunostaining of *optoA$_{2A}$R*-expressing cells before and after light stimulation. (**e**) Western blot analysis of p-MAPK and MAPK expression in response to light. (**f** and **h**) Light-induced increase of cAMP (**f**; plasmid: $F(1,62) = 126.7$, $P < 0.001$; light stimulation, $F(1,62) = 67.8$, $P < 0.001$; plasmid × light, $F(1,62) = 89.4$, $P < 0.001$, two-way analysis of variance (ANOVA)) but not of cGMP (**g**; light, $F(1,62) = 0.110$, $P > 0.05$, two-way ANOVA) or IP_1 production (**h**; light, $F(1,62) = 0.110$, $P > 0.05$, two-way ANOVA) in HEK293 cells transfected with *optoA$_{2A}$R*. $^{***}P < 0.001$, comparing *optoA$_{2A}$R* with control; $^{###}P < 0.001$ compared with the dark, $n = 16$, two-way ANOVA, Bonferroni *post hoc t*-test. (**i**) Effect of the mutations Ser400Ala and Thr324Ala of the C terminal of *optoA$_{2A}$R* on light *optoA$_{2A}$R*-induced cAMP accumulation. $^{**}P < 0.01$, Student's *t*-test. (**j**) Time course of *opto-A$_{2A}$R*-induced cAMP accumulation after light stimulation. One-way ANOVA, Bonferroni *post hoc t*-test. Each experiment was carried out in duplicates or triplicates and repeated at least three times. Scale bar = 50 μm.

3000 light pulses (465 nm, 50 ms pulse width, ~3–5 mW mm^{-2} power density) during a total period of 300 s, applied through a Plexibright LD-1 LED module with a 465 nm Blue (Plexon, Dallas, TX, USA) and the optic fiber was placed over the slice between the stimulation and recording electrodes. Light stimuli were triggered 300 s before the delivery of the HFS protocol. The A2AR agonist CGS21680 (30 nM; Tocris, Ballwin, MO, USA) was added to the superfusion solution at least 20 min before the HFS protocol onwards. LTP amplitude was quantified as the percentage change between two values: the average slope of the five potentials taken between 50 and 60 min after the induction protocol in relation to the average slope of the field excitatory postsynaptic potentials measured during 15 min that preceded the induction protocol.

Optogenetic activation of *optoA$_{2A}$R* signaling in the brain

A 200 μm core fiber (ThorLabs, Newton, NJ, USA) was used for optical stimulation via a patch cable connected to a 473 nm DPSS laser (100 mW; Shanghai Laser & Optics Century, Shanghai, China). The power density at the fiber tip was ~3–5 mW mm^{-2} and light was delivered with 50 ms pulse width. For assessment of *optoA$_{2A}$R* signaling, mice were killed following 10 min optical stimulation. For behavior assessments, optical stimulation was delivered specifically according to different behavioral test (see below).

Behavioral tests

For the open-field test, mice were placed in the center of a white, dimly light open-field chamber (40×40 cm^2) and allowed to freely explore the environment. The center of the open-field was defined as >10 cm apart from all four walls. 'Off-On-Off' episodes of light stimulation were used and each block lasted 5 min, for a total of 15 min. Locomotor activity was detected with a video camera and analyzed with ANY-maze Video Tracking System (Stoelting, Wood Dale, IL, USA). The Y-maze test for recognition memory task was based on exploration of novelty as described previously.[34] The test consisted of two trials, separated by a 1-h time interval. During the first trial (acquisition phase), one arm of the Y-maze was closed and mice were allowed to explore the remaining two arms for 10 min with light 'OFF', with several visual clues on the walls of the room. During the second trial (retrieval phase), the mice had access to the three arms for a 5-min period with light 'ON'. During this period, the time spent in each arm and the total locomotor activity of each mouse was measured by a video-tracking system (Smart; Bioseb Chaville, Chaville, France).

Immunohistochemistry

Following agonist injection or light stimulation, mice were transcardially perfused with ice-cold 4% paraformaldehyde in PBS (pH 7.4) after termination of the light stimulation. Brains were postfixed and coronal sections with 30–40 μm were cut and processed for immunohistochemistry. Free-floating sections were washed in PBS and then incubated for 30 min in 0.3% Triton X-100 and 3% normal donkey or goat serum. Primary antibody incubations were conducted overnight in 0.01% Triton X-100 and 3% normal donkey serum for A_{2A}R (Santa Cruz; 1:200), p-MAPK (Cell Signaling; 1:200), p-CREB (Cell Signaling; 1:200) or c-fos (Santa Cruz; 1:300). Sections were then washed with PBS and incubated for 1 h at room temperature with Alexa Fluor 488-conjugated secondary antibodies (Molecular Probes; 1:200). Slices were then washed and mounted on slides with Vectashield mounting media (Vector Laboratories). Images were acquired with a fluorescence microscope.

Preparations of total membranes and synaptosomes

Total membranes and synaptosomes from the hippocampus were prepared using sucrose/Percoll differential centrifugations, as described previously.[35] Briefly, two mouse hippocampi were placed in ice-cold 0.32 M sucrose solution and instantly homogenized with a Teflon homogenizer. After centrifugation at 3000 *g* for 10 min, the supernatant was collected and divided to prepare synaptosomes or total membranes. To prepare total membranes, the supernatant was centrifuged at 28000 *g* for 60 min and the pellet was collected. To prepare synaptosomes, the supernatant was centrifuged at 14 000 *g* for 12 min and the pellet was resuspended in 1 ml of a solution of 45% (v v^{-1}) Percoll in Krebs solution. After centrifugation, the top layer (synaptosomal fraction) was removed and washed with 1 ml ice-cold Krebs solution. The synaptosomes or total membranes were further resuspended in radioimmunoprecipitation assay buffer supplemented with a cocktail of protease inhibitors (Roche, Basel, Switzerland) for western blot analysis or in Krebs solution for immunocytochemical analysis.

Western blot analysis

Western blot analysis was carried out as described previously.[35] Briefly, after determining the amount of protein, total membrane or synaptosomal samples were diluted with five volumes of sodium dodecyl sulfate-polyacrylamide gel electrophoresis buffer. These diluted samples were separated by sodium dodecyl sulfate-polyacrylamide gel electrophoresis (10% with a 4% concentrating gel) under reducing conditions and electrotransferred to nitrocellulose membranes (Amersham Biosciences, Piscataway, NJ, US). After blocking for 1 h at room temperature with 5% milk in Tris-buffered saline (pH 7.6) containing 0.1% Tween-20 (TBS-T), the membranes were incubated overnight at 4 °C with a rabbit anti-A_{2A}R antibody (1:500, 05-717; Millipore). After three washing, the membranes were incubated with horseradish peroxidase goat anti-mouse secondary antibody (1:1500; Pierce, Rockford, IL, USA) in TBS-T during 120 min at room temperature. After three washes, the membranes were incubated with Luminata Forte (Millipore) during 5 min and then analyzed with a VersaDoc 3000 (Bio-Rad, Amadora, Portugal) to quantify A2AR immunoreactivity as well as mCherry fluorescence. The membranes were then reprobed and normalized for α-tubulin (1:20 000; Sigma, St. Louis, MO, USA) immunoreactivity.

Immunocytochemistry of synaptosomes

The immunocytochemical analysis of hippocampal synaptosomes, to detect the presence of *optoA$_{2A}$R* in glutamatergic terminals, was carried out as reported previously.[36] The synaptosomes were placed onto coverslips coated with poly-D-lysine, fixed with 4% paraformaldehyde in PBS for 15 min and washed two times with PBS. The synaptosomes were permeabilized in PBS with 0.2% Triton X-100 for 10 min and then blocked for 1 h in PBS with 3% bovine serum albumin and 5% normal bovine serum. The synaptosomes were incubated overnight at 4°C with either a mouse anti-A_{2A}R antibody (1:500; 05-717; Millipore) or with a guinea-pig vesicular glutamate transporters type-1 antibody (1:2500; 135304; Synaptic Systems, Göttingen, Germany), followed by incubation of donkey Alexa Fluor-488-conjugated anti-mouse IgG (alone) and goat Alexa Fluor-488-conjugated anti-guinea-pig IgG (1:1000; Molecular Probes). The colocalization of vesicular glutamate transporters type-1 or A_{2A}R immunoreactivities with mCherry fluorescence was examined under a Zeiss Imager Z2 fluorescence microscope (Zeiss, Gottingen, Germany) and analyzed with ImageJ 1.37v software (NIH, Bethesda, MD, USA), as described previously.[37]

Statistics

Results are presented as mean ± s.e.m. Data with one variable and one condition (e.g. light stimulation in Figures 1j and 3; AAV/plasmid vector in Figures 4d, e and 5e, f) were analyzed with Student's *t*-test. Data from one variable with more than one condition (e.g. multiple time courses in Figure 1i) were analyzed with one-way analysis of variance (ANOVA), followed by Bonferroni *post hoc* comparison. Data with more than one variable (e.g. AAV vectors and light stimulation in Figures 2f–h; CGS21680 and light stimulation in Figures 2a–c; AAV vectors and behavioral phase in Figures 4f and 5g) and condition were analyzed with two-way ANOVA and Bonferroni *post hoc* tests.

RESULTS

Light activation of *optoA$_{2A}$R* specifically recruits A_{2A}R signaling in HEK293 cells

We engineered a light-activated chimeric protein able to recruit A_{2A}R signaling, *optoA$_{2A}$R*, by replacing the intracellular domains of rhodopsin with those of A_{2A}R (Figure 1a). At 24 h after transfecting HEK293 cells with *optoA$_{2A}$R*, we observed a single band with a 80 kDa molecular weight, expected for *optoA$_{2A}$R* (Figure 1b), using an A_{2A}R antibody targeting the third *intracellular* loop of A_{2A}R. We also detected the red fluorescence of mCherry, included in the *optoA$_{2A}$R* construct, largely restricted to the cell surface (Figure 1c), similar to that obtained using the A_{2A}R antibody.

A_{2A}R activate the G_S/G_{olf}-cAMP pathway as well as MAPK pathway in a G_S-independent manner.[25] Light stimulation of HEK293-*optoA$_{2A}$R* cells (for 60 s) increased p-MAPK, in contrast with the weak p-MAPK immunoreactivity in light-stimulated cells transfected with the pcDNA3.1 vector (Figure 1d), which was confirmed by western blot (Figure 1e). Light stimulation of HEK293-*optoA$_{2A}$R* cells also increased cAMP levels by twofold (immunoassay after 20 min), compared with non-stimulated HEK293-*optoA$_{2A}$R* cells and with light-stimulated cells transfected with pcDNA3.1 (Figure 1f; $P < 0.001$, two-way ANOVA). Thus, *optoA$_{2A}$R* specifically recruits the two parallel A_{2A}R signaling pathways, namely G_S-cAMP and MAPK signaling, in HEK293 cells.

Supporting the specificity of *optoA$_{2A}$R* signaling, light stimulation of HEK293-*optoA$_{2A}$R* cells induced cAMP and p-MAPK signaling (Figures 1e and f) but did not affect either cGMP (the

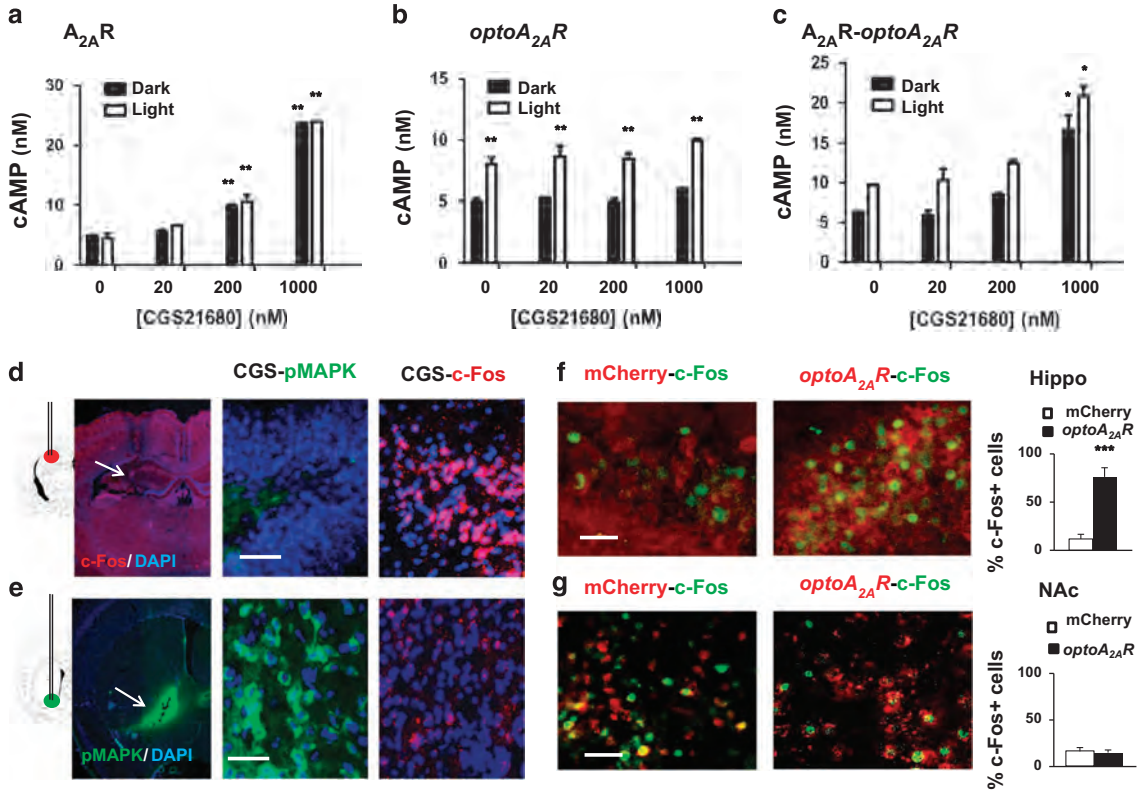

Figure 2. *OptoA$_{2A}$R* and CGS21680 produced additive induction of cAMP in human embryonic kidney 293 (HEK293) cells and indistinguishable biased A_{2A}R signaling in the nucleus accumbens (NAc) and hippocampus. (**a–c**) HEK293 cells were transfected with wild-type A_{2A}R (**a**) or *optoA$_{2A}$R* (**b**) or co-transfected with wild-type A_{2A}R and *optoA$_{2A}$R* (**c**). (**a**) At 24 h after transfection, cells transfected with wild-type A_{2A}R were treated with the A_{2A}R agonist CGS21680 (20, 100, 200 and 1000 nM) and displayed a concentration-dependent increase of cAMP levels. Light activation of *optoA$_{2A}$R*-transfected HEK293 cells increased cAMP levels (**b**; for light, $F(1,31) = 60.721$, $P < 0.001$; for CGS21680, $F(3,31) = 2.163$, $P > 0.05$; lightxCGS21680 interaction, $F(3,31) = 0.155$, $P > 0.05$, two-way analysis of variance (ANOVA)) similar to that induced by 200 nM CGS21680 (**a**; for light, $F(1,46) = 0$, $P > 0.05$; for CGS21680, $F(3,46) = 312.799$, $P < 0.001$; lightxCGS21680 interaction, $F(3,46) = 0.547$, $P > 0.05$, two-way ANOVA). Costimulation of light and CGS21680 in cells co-transfected with *optoA$_{2A}$R* and wild-type A_{2A}R produced an additive effect on cAMP levels (**c**; for light stimulation, $F(1,43) = 7.243$, $P < 0.01$; for CGS21680, $F(3,43) = 32.674$, $P < 0.001$; lightxCGS21680 interaction, $F(3,45) = 0.336$, $P > 0.05$, two-way ANOVA). $^{*}P < 0.05$, $^{**}P < 0.01$, two-way ANOVA, Bonferroni *post hoc* *t*-test. Following intra-accumbal injection, CGS21680 markedly induced phospho-mitogen-activated protein kinase (p-MAPK) expression (green) but not c-Fos expression around the injection site (**d**, lower panel). Following intrahippocampal injection, CGS21680 induced c-Fos expression (right) but not p-MAPK expression (left) around the injection site (**e**, upper panel). (**f** and **g**) Two weeks after intrahippocampal injection of AAV5-*optoA$_{2A}$R*, light stimulation for 5 min induced c-Fos expression in *optoA$_{2A}$R*-positive cells but not in cells transfected with AAV5-mCherry (3 fields per section, 3 sections per mouse, 3 mice per group). $^{***}P < 0.001$, Student's *t*-test comparing the optoA$_{2A}$R with the mCherry. Scale bar = 50 μm (**d–g**).

rhodopsin transducing system; Figure 1g) or IP1 production (a degradation product of IP3, associated with G_q signaling; Figure 1h). Further reinforcing the selectivity of *optoA$_{2A}$R* to trigger cAMP accumulation, a Ser400Ala point mutation in an A_{2A}R phosphorylation site critical for A_{2A}R–D_2R receptor interaction,[38] but not a Thr324Ala point mutation in an A_{2A}R phosphorylation site critical for short-term desensitization,[30] of the C terminals of *optoA$_{2A}$R* abolished the light *optoA$_{2A}$R*-induced cAMP accumulation (Figure 1i; $^{**}P < 0.01$, Student's *t*-test). Thus, *optoA$_{2A}$R* signaling is specific and attributed to the unique amino-acid composition of its C terminus. Lastly, light stimulation of *optoA$_{2A}$R* rapidly increased cAMP and p-MAPK levels in HEK293 cells within 1 min, peaking at 15–30 min and declining to basal level at 60–90 min (Figure 1j; $P < 0.05$, one-way ANOVA).

Light *optoA$_{2A}$R* activation triggers an A_{2A}R signaling identical to the pharmacological activation of endogenous A_{2A}R both in HEK293 cells and mouse brain

To demonstrate the physiological relevance of *optoA$_{2A}$R* signaling, we first compared cAMP levels and p-MAPK induced by either light activation of *optoA$_{2A}$R* or CGS21680 (A_{2A}R agonist) activation of wild-type A_{2A}R in HEK293 cells. Light *optoA$_{2A}$R* activation increased cAMP (Figure 2b; $P < 0.001$, two-way ANOVA) to levels similar to those triggered by CGS21680 (200 nM) in cells transfected with A_{2A}R-mCherry (Figure 2a; $P < 0.001$, two-way ANOVA). Moreover, in cells co-transfected with A_{2A}R-mCherry and *optoA$_{2A}$R*, costimulation with light and CGS21680 produced additive effects on both cAMP level (Figure 2c; light, $F(1,43) = 7.243$, $P < 0.01$; CGS21680, $F(3,43) = 32.674$, $P < 0.001$; lightxCGS21680 interaction, $F(3,43) = 0.336$, $P > 0.05$, two-way ANOVA) and p-MAPK. Thus, *optoA$_{2A}$R* and CGS21680 produced similar A_{2A}R signaling with additive effects in HEK293 cells.

We further compared A_{2A}R signaling (c-Fos and p-MAPK) in the hippocampus and NAc induced by endogenous A_{2A}R activation in wild-type mice and by *optoA$_{2A}$R* in transfected A_{2A}R knockout mice. Intrahippocampal injection of CGS21680 (0.93 nmol μl^{-1}) significantly increased c-Fos expression within 15 min specifically in the cells surrounding the injection site (Figure 2d). By contrast, intra-accumbal injection of CGS21680 markedly induced p-MAPK (Figure 2e). Thus, endogenous A_{2A}R activation elicits a brain region-specific A_{2A}R signaling in the forebrain (c-Fos in the hippocampus and p-MAPK in the NAc). Accordingly, light *optoA$_{2A}$R*

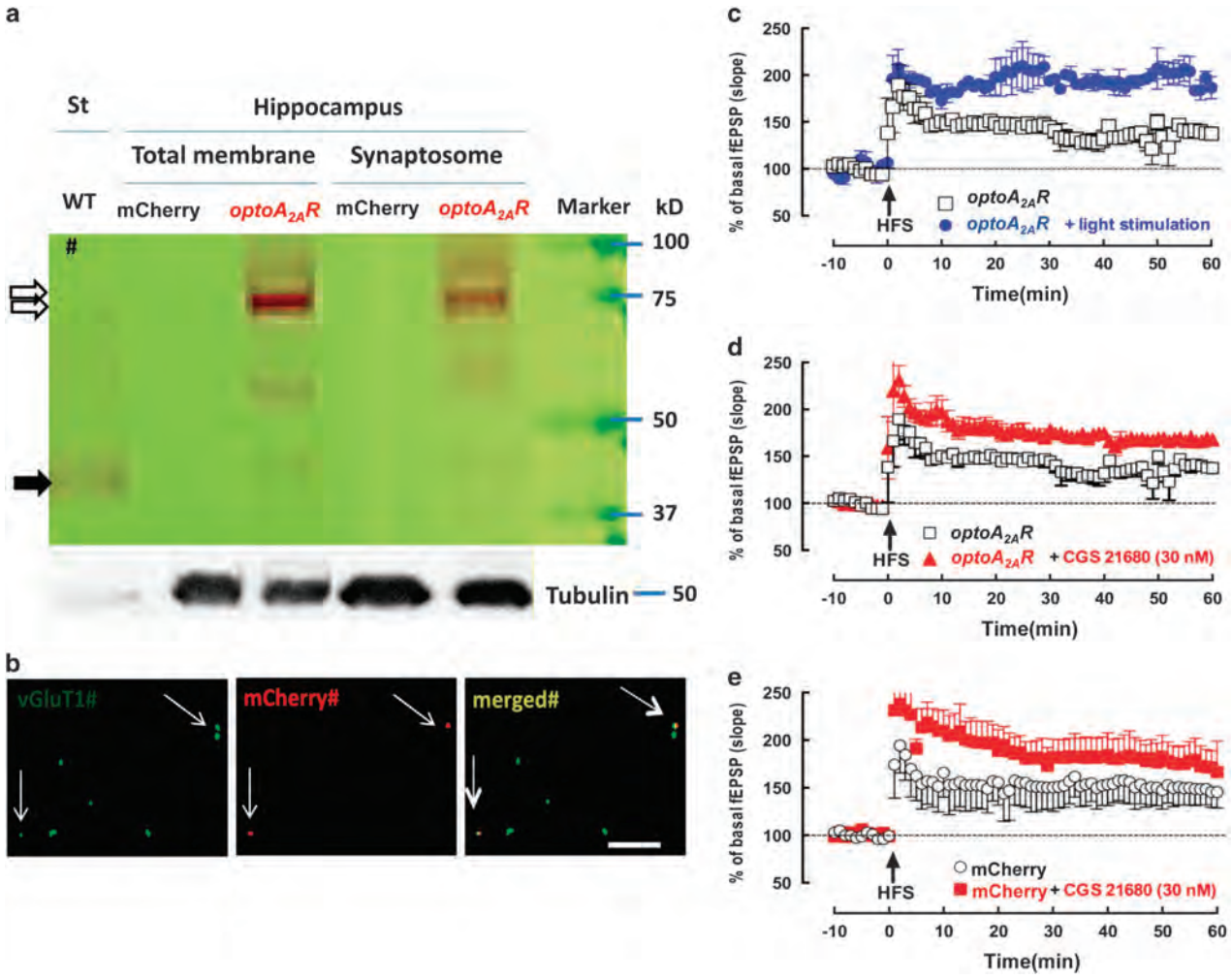

Figure 3. Targeted expression and light activation of *optoA$_{2A}$R* in glutamatergic terminals of the hippocampus induced hippocampal long-term potentiation (LTP) in brain slices. (**a**) Representative western blot analysis showing that an antibody against the third intracellular loop of A_{2A}R recognized two bands at 80 and 95 kDa in hippocampal synaptosomes as well as in total membranes from mice transfected with AAV-mCherry-*optoA$_{2A}$R* (*optoA$_{2A}$R*) but not from mice transfected with AAV-mCherry, compatible with the localization of *optoA$_{2A}$R* in hippocampal synapses ($n = 3$). (**b**) Representative single nerve terminal immunocytochemistry identifying that vesicular glutamate transporter type-1 (vGluT1, a marker of glutamatergic terminals; green) and mCherry immunoreactivity (red) were found to be colocalized (arrows identifying yellow in 'merged') in hippocampal synaptosomes from mice transfected with AAV-mCherry-*optoA$_{2A}$R* (*optoA$_{2A}$R*), whereas this was not observed for mice transfected with AAV-mCherry (not shown) ($n = 3$). (**c**) Accordingly, light stimulation (3000 pulses of 50-ms duration each during 300 s) of slices from mice transfected with AAV-mCherry-*optoA$_{2A}$R*, applied before a high-frequency train (100 Hz for 1 s), enhanced the amplitude of LTP compared with non-light-stimulated slices, measured as an increased slope of field excitatory postsynaptic potentials (fEPSP) recorded in the *stratum radiatum* of the CA1 area upon stimulation of the afferent Schaffer fibers (**c**), whereas light stimulation failed to modify LTP amplitude in mice transfected with AAV-mCherry (not shown). This essentially mimics the effect of the pharmacological activation of endogenous A_{2A}R with the selective A_{2A}R agonist CGS21680 (30 nM), in slices from mice transfected either with AAV-mCherry-*optoA$_{2A}$R* (**d**) or with AAV-mCherry (**e**). Representative images (**a** and **b**) and data (mean ± s.e.m., **c–e**) are from $n = 3$ independent mice. *$P < 0.05$, Student's *t*-test.

stimulation in the hippocampus significantly increased c-Fos expression specifically in the *optoA$_{2A}$R*-expressing cells underneath the cannula (Figure 2f), whereas *optoA$_{2A}$R* activation in NAc markedly induced p-MAPK but not c-Fos (Figure 2g). This demonstrates a similarly biased A_{2A}R signaling triggered by *optoA$_{2A}$R* and CGS21680, that is, c-Fos in the hippocampus and p-MAPK in the NAc, supporting the ability of *optoA$_{2A}$R* to mimic the endogenous A_{2A}R signaling in the brain.

Targeted expression and light activation of *optoA$_{2A}$R* in glutamatergic terminals of the hippocampus controlling LTP in hippocampal slices

The A_{2A}R antibody detected a single 45 kDa band (endogenous A_{2A}R) in striatal membranes, whereas A_{2A}R levels were barely detectable in hippocampal samples, compatible with the 20 times lower density of A_{2A}R in the hippocampus vs the striatum. Importantly, this A_{2A}R antibody designed against the third intracellular loop of A_{2A}R recognized two bands of 80 and 95 kDa selectively in the hippocampus transfected with AAV-mCherry-*optoA$_{2A}$R* but not with AAV-mCherry (Figure 3a), with a density in synaptosomes similar to that detected in total membranes ($n = 3$, $P > 0.05$, Student's *t*-test). Furthermore, the immunocytochemistry analysis of purified synaptosomes (Figure 3b) allowed the identification of mCherry fluorescence in glutamatergic nerve terminals (i.e. immunopositive for vesicular glutamate transporters type-1) only from the hippocampus transfected with AAV-mCherry-*optoA$_{2A}$R* ($n = 3$) but not with AAV-mCherry (not shown). This indicates that *optoA$_{2A}$R* is present in hippocampal

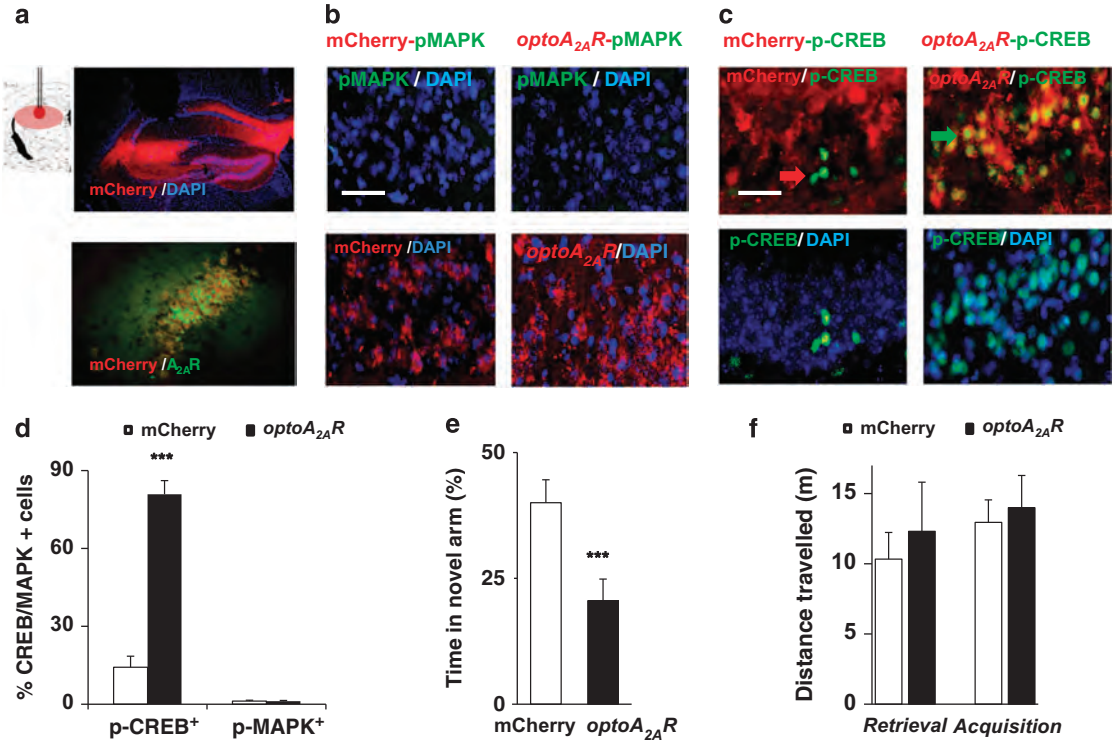

Figure 4. Light activation of hippocampal *optoA$_{2A}$R* triggers CREB phosphorylation and memory impairment. (**a**) Upper panel: Schematic illustration of transplanted cannula targeting hippocampus and expression of mCherry (*optoA$_{2A}$R)* under CaMKIIa promoter in the hippocampus after focal injection of AAV5-*optoA$_{2A}$R*-mCherry (AP, − 2.2 mm; ML, ± 1.5 mm; DV, +2.3 mm). Lower panel: colocalization of A_{2A}R immunostaining (green) with mCherry-expressing (red) in *optoA$_{2A}$R*-expressing cells. (b and **c**) Light stimulation of *optoA$_{2A}$R* in the hippocampus for 5 min induced phospho-CREB (p-CREB) (b and **d**) but not phospho-mitogen-activated protein kinase (p-MAPK) (**c** and **d**) ($P = < 0.001$, Student's *t*-test) in *optoA$_{2A}$R*-positive cells but not in cells transfected with AAV5-mCherry (3 fields per section, 3 sections per mouse, 3 mice per group). (**e**) Light stimulation of *optoA$_{2A}$R* signaling in the hippocampus during the retrieval phase impaired spatial recognition memory with decreased time in the novel arm ($P \leqslant 0.001$, Student's *t*-test) of the Y-maze but had no effect on total distance travelled (**f**; AAV vector ($F(1,41) = 0.45$, $P > 0.05$, two-way analysis of variance (ANOVA)) during on the 5-min 'Light-On' period, compared with that of the control. Green arrow: colocalization of *optoA$_{2A}$R* with p-CREB; red arrow: p-CREB expression only. Scale bar = 50 μm.

glutamatergic nerve terminals, where endogenous A_{2A}R have been identified.

Additionally, we observed (Figure 3c) that the amplitude of LTP triggered by HFS was larger upon light stimulation (5 min before HFS) of hippocampal slices expressing *optoA$_{2A}$R* (197.3 ± 2.9% over baseline) than without light stimulation (137.7 ± 2.0% over baseline, $n = 3$; $P > 0.05$, Student's *t*-test). By contrast, light stimulation did not modify LTP amplitude in hippocampal slices expressing only mCherry (138.9 ± 2.7% vs 142.5 ± 1.5% over baseline with or without light stimulation, respectively, $n = 3$; $P > 0.05$, Student's *t*-test) (data not shown). This enhancement upon light-induced *optoA$_{2A}$R* activation was similar to the impact of a pharmacological activation of endogenous A_{2A}R with the A_{2A}R agonist, CGS21680 (30 nM) (Figure 3d) , as well as in slices from mice transfected with AAV-mCherry (Figure 3e), as occurs in the wild-type animals. This shows that light activation of *optoA$_{2A}$R* can mimic an established physiological response operated by endogenous A_{2A}R in the hippocampus.[39]

Optogenetic *optoA$_{2A}$R* activation in the hippocampus recruits CREB phosphorylation and impairs memory performance

Two weeks after the focal injection of AAV5-(CaMKIIα promoter-driven)-*optoA$_{2A}$R*-mCherry (Figure 4a), light stimulation in the dorsal hippocampus significantly increased the levels of p-CREB (Figures 4c and d; $P < 0.001$, Student's *t*-test) specifically in the *optoA$_{2A}$R*-expressing neurons underneath the cannula, consistent with the A_{2A}R-G_S-cAMP pathway as the major A_{2A}R signaling pathway in the hippocampus.[25] Similar to p-CREB recruitment, light stimulation significantly elevated c-Fos in the *optoA$_{2A}$R*-expressing neurons in hippocampus (Figure 2f; $P < 0.001$, Student's *t*-test), whereas it did not induce p-MAPK (Figures 4b and d). Thus, in hippocampal neurons, light *optoA$_{2A}$R* activation preferentially stimulates the cAMP-PKA pathway, leading to p-CREB and c-Fos expression, without significant effect on the p-MAPK pathway.

To address the central question whether A_{2A}R activation in the hippocampus is sufficient to impair memory performance, we tested if triggering hippocampal *optoA$_{2A}$R* signaling affected spatial reference memory performance using a two-visit version of the Y-maze test. Light *optoA$_{2A}$R* activation in the hippocampus during the 5-min testing period reduced about twofold the time spent in the novel arm compared with mice transfected with AAV-mCherry (control) only (Figure 4e; $P < 0.001$, Student's *t*-test). These short-term reference memory impairments were not due to changes in locomotion as gauged by the unaltered total distance travelled in the Y-maze (Figure 4f). Thus, *transient* activation of *optoA$_{2A}$R* in a set hippocampal neurons is sufficient to recruit p-CREB signaling and deteriorate memory performance.

Light *optoA$_{2A}$R* stimulation in NAc recruits MAPK phosphorylation and selectively modulates motor activity

We next examined the impact of light *optoA$_{2A}$R* activation in the NAc and the hippocampus on the two A_{2A}R signaling pathways

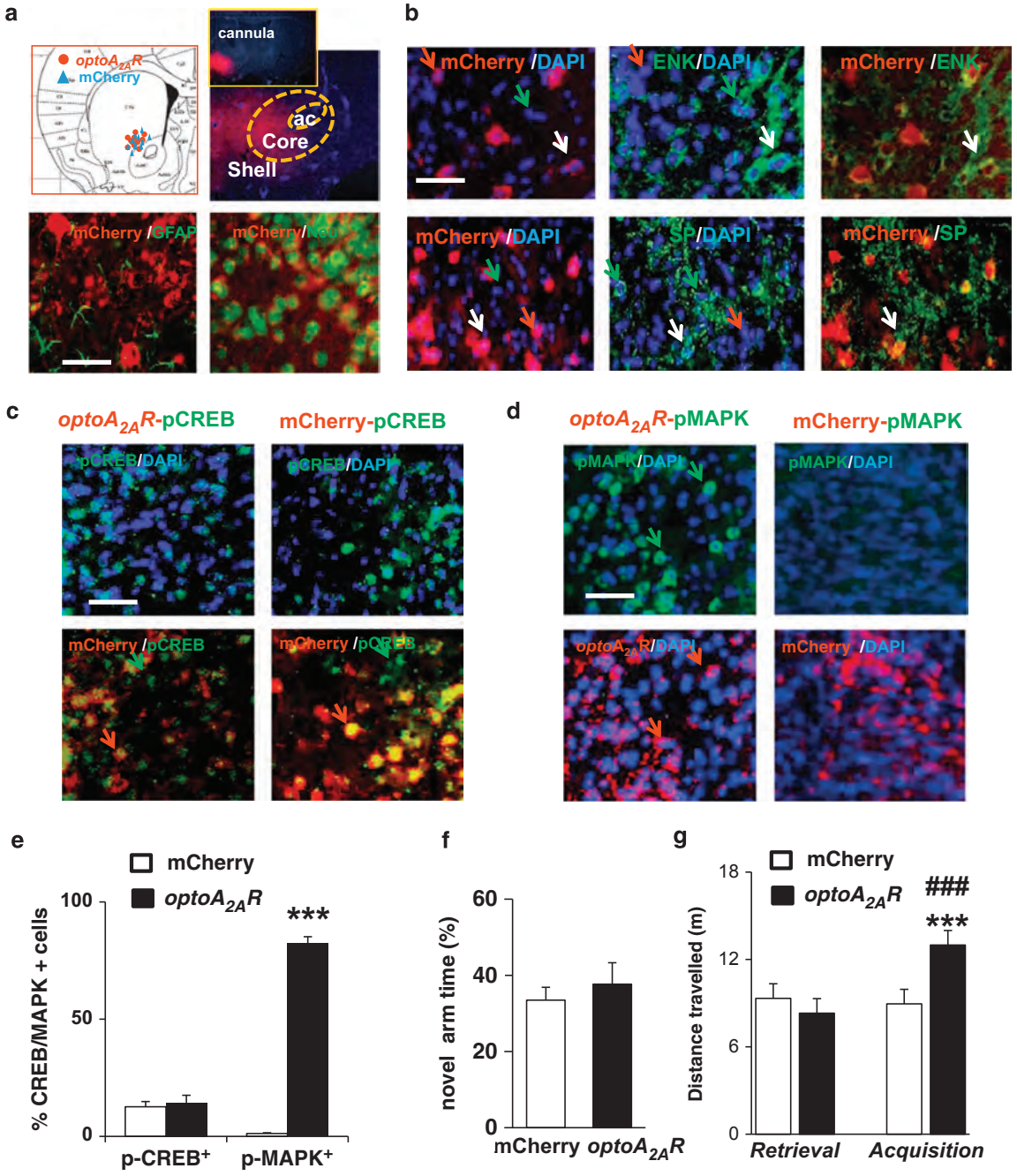

Figure 5. Light activation of accumbal *optoA$_{2A}$R* triggered phospho-mitogen-activated protein kinase (p-MAPK) phosphorylation and locomotor response. (**a**) Top left: Schematic illustration and mCherry (*optoA$_{2A}$R)* under CaMKIIa promoter in nucleus accumbens (NAc) after focal injection of AAV5-*optoA$_{2A}$R*-mCherry in the NAc (AP, +1.1 mm; ML, ± 1.4 mm; DV, +4.5 mm). Top left: Schematic illustration and location of mCherry in the core and shell of NAc. Top right: A_{2A}R immunostaining (green) localized in mCherry-expressing (red) *optoA$_{2A}$R*–positive cells. Bottom left: *optoA$_{2A}$R*-mCherry were colocalized in NeuN-positive (green) but not GFAP-positive cells. (**b**) Expression of *optoA$_{2A}$R* in enkephalin (ENK)-positive and substance P (SP)-positive medium-sized spiny neurons. (**c** and **d**) Light induction of phospho-CREB (p-CREB) (**c**) and p-MAPK (**d**) (green) in the NAc at 2 weeks after intra-NAc injection of AAV5-*optoA$_{2A}$R* (right) or AAV5-mCherry (left). Light stimulation produced scattered expression of p-CREB but triggered a robust induction of p-MAPK with mCherry-expressing in *optoA$_{2A}$R*-positive cells (right panels). (**e**) Quantitative analysis of light induction of p-CREB and p-MAPK in *optoA$_{2A}$R*-positive cells but not in cells transfected with AAV5-mCherry. p-CREB/p-MAPK-positive cell accounts were obtained from 3 fields per section, 3 sections per mouse and 3 mice per group. $^{***}P < 0.001$, Student's *t*-test comparing the optoA$_{2A}$R with the mCherry. (**f** and **g**) Light stimulation of *optoA$_{2A}$R* in the NAc increased the total distance travelled at the acquisition phase (**g**; for AAV vector, $F(1, 44) = 10.11$, $P < 0.003$; for behavioral phase, $F(1,44) = 25.08$, $P < 0.001$; AAV vectorxbehavioral phase, $F(1,44) = 18.68$, $P < 0.001$, two-way analysis of variance (ANOVA); $^{***}P < 0.001$, $^{###}P < 0.001$, Bonferroni *post hoc* test, comparing *optoA$_{2A}$R* with mCherry) but had no effect time spent in the novel arm during the 5-min 'Light-On' period, compared with that of the mCherry (**f**; $P = 0.276$, Student's *t*-test). Scale bar = 50 μm. Green arrow: colocalization of *optoA$_{2A}$R* with p-CREB; red arrow: p-CREB expression only; white arrow: colocalization of *optoA$_{2A}$R* with ENK, SP, p-CREB or phospho-MAPK; green arrow: ENK, SP, p-CREB or phospho-MAPK only; red arrow: mCherry expression only.

(p-CREB and p-MAPK). As GPCR can produce a biased signaling simply due to different receptor levels, we used the same CaMKIIα promoter to drive similar levels of *optoA$_{2A}$R* expression in hippocampal and striatal neurons,[40,41] to eliminate different *optoA$_{2A}$R* expression levels as a possible cause of a biased A_{2A}R signaling in these two forebrain regions.[42] *OptoA$_{2A}$R* was selectively expressed in accumbal neurons (colocalized with Neu+ neurons but not with GFAP+ astrocytes) in the core of NAc (Figure 5a). Using enkephalin (ENK) and substance P immunostaining to identify the indirect and direct pathway neurons,[43] we found that *optoA$_{2A}$R* was expressed in both ENK- (52%) and SP-containing (43%) neurons in NAc (Figure 5b). Importantly, light activation of *optoA$_{2A}$R* in NAc for 5 min markedly increased p-MAPK (Figures 5d and e; $P < 0.001$, Student's *t*-test), with little induction of p-CREB and c-Fos (Figures 5c, e and 2g). Thus, the activation of A_{2A}R signaling by *optoA$_{2A}$R* in NAc preferentially involved the MAPK pathway rather than the cAMP-PKA-mediated c-Fos/CREB pathway.

In parallel with the preferential activation of p-MAPK signaling, light *optoA$_{2A}$R* activation in NAc for 5 min did not affect memory performance in the modified Y-maze test (Figure 5f; $P = 0.276$, Student's *t*-test), but robustly increased locomotor activity (83% increase of travelled distance in the Y-maze, Figure 5g, and in the open-field test) (for AAV vectorxbehavioral phase, $F(1,45) = 18.68$, $P < 0.001$, two-way ANOVA). The observed motor stimulant effect resulting from *optoA$_{2A}$R* activation in the NAc, instead of a motor depression observed upon accumbal administration of CGS21680,[44,45] was expected in view of the expression of *optoA$_{2A}$R* in both striatopallidal and striatonigral neurons using the CaMKIIα promoter[41,42] (rather than the selective expression of endogenous A_{2A}R in striatopallidal neurons prompted by the A_{2A}R promoter[46]). This pitfall was however essential to circumvent the confounding effect of a 20-fold differential expression of A_{2A}R in these two brain regions as a possible cause for the biased A_{2A}R signaling. Overall, the present findings show that A_{2A}R trigger a biased A_{2A}R signaling in different forebrain regions (cAMP in the hippocampus and p-MAPK in the NAc) in parallel with an impact on distinct behaviors (memory in the hippocampus and locomotion in NAc).

DISCUSSION

The development and validation of the *optoA$_{2A}$R* approach to mimic endogenous A_{2A}R signaling allowed the novel conclusion that the recruitment of A_{2A}R signaling in the dorsal hippocampus is sufficient to trigger a selective memory deficit. This is in accordance with the imbalance of the local extracellular adenosine levels[21] and upregulation of A_{2A}R in animal models of aging,[47] sporadic dementia[11] and AD,[10] as well as in the human AD brain,[48] namely in hippocampal nerve terminals,[12,13] a situation that was mimicked by hippocampal *optoA$_{2A}$R* expression under the control of the CaMkIIα promoter. Indeed, *optoA$_{2A}$R* was detected in hippocampal synaptosomes, namely in glutamatergic synapses where endogenous A_{2A}R are identified and upregulated upon aging and neurodegeneration. This provides an anatomical basis for *optoA$_{2A}$R* control of p-CREB signaling, synaptic activity and memory performance. Indeed, the light activation of *optoA$_{2A}$R* in hippocampal slices mimicked a well-established physiological response operated by endogenous A_{2A}R, the control of hippocampal LTP.[39] Furthermore, optoA$_{2A}$R activation in the hippocampus triggers CREB phosphorylation and impairs memory performance. These findings are consistent with the canonical cAMP/PKA pathway activated by hippocampal A_{2A}R[25] and with the established role of CREB phosphorylation controlling synaptic plasticity and long-term memory[49] through neuronal excitability and transcription, and with specific deficits of memory retrieval observed in mice expressing a time-controlled active CREB variant.[39] This ability of hippocampal *optoA$_{2A}$R* activation in glutamate synapses to control memory dysfunction and its purported neurophysiological correlate LTP, decisively strengthens the relation between A_{2A}R and memory performance that had so far largely relied on the demonstration that A_{2A}R blockade alleviated memory dysfunction.[8,9,12,14,15] Furthermore, this ability to place A_{2A}R functioning as a sufficient factor to imbalance memory bolsters the rationale to probe the therapeutic effectiveness of A_{2A}R antagonists to manage memory impairment.[22,23] This notion is further warranted by the striking convergence of epidemiological[1–7] and animal[8–20] evidence supporting the therapeutic benefit of caffeine and A_{2A}R antagonists to improve cognition. This aim should be facilitated by the safety profile of A_{2A}R antagonists, tested in over 3000 parkinsonian patients.[22]

The design of *optoA$_{2A}$R* also allowed identifying a critical role solely attributable to the intracellular domains of A_{2A}R to dictate the biased A_{2A}R signaling and function in neurons of different brain regions. Contrary to the widely accepted view that ligand–receptor interactions are the molecular basis directing the biased GPCR signaling, the distinct molecular and behavioral responses obtained upon *optoA$_{2A}$R* activation in different brain regions show that they are only dependent on an intracellular mechanism probably related with the differential association with different GIPs in different cell types. In fact, the cell-specific expression of intracellular GIPs provides a rich molecular resource[50] whereby A_{2A}R signaling in the brain is specifically wired according to the needs of each cell type. In particular, the long and flexible A_{2A}R C terminus[29] contains several consensus sites (e.g. YXXGφ)[30] required for MAPK activation,[51] interaction with BDNF receptors (TrkB),[52] with FGF,[53] p53,[54,55] with a large set of downstream signaling effectors such as G proteins, GPCR kinases, arrestins and with at least six GIPs (actinin, calmodulin, Necab2, translin-associated protein X, ARNO/cytohesin-2, ubiquitin-specific protease-4).[29] Thus, targeting A_{2A}R intracellular domains offers an additional layer of selectivity to manipulate A_{2A}R signaling that is not attainable only by the ligand–receptor interaction. Thus, selectively targeting A_{2A}R intracellular domains and their interacting GIPs in specific brain regions emerges as a novel strategy to obtain therapeutic effects with minimal side effects, as achieved with transmembrane peptides to disrupt specifically the intracellular interaction between NMDA receptors and PSD95[56,57] and between 5-HT2c-PENT.[58] If the critical interaction between intracellular domains of A_{2A}R and GIPs are general features of GPCRs, the '*optoGPCR*' approach targeting intracellular domains of GPCRs may represent a novel drug discovery strategy for the largest protein superfamily in the human genome.

The significance of these novel insights is decisively strengthened by the demonstrated specificity and rapid induction of the *optoA$_{2A}$R* signaling. The specificity of *optoA$_{2A}$R* signaling is supported by the selective optogenetic induction of cAMP and MAPK signaling without affecting cGMP (rhodopsin) and IP3 (G_q) signaling and by the mutational analysis demonstrating that *optoA$_{2A}$R* signaling is specifically attributed to the unique amino-acid composition of the A_{2A}R C terminus. Moreover, the comparable activation of A_{2A}R signaling in HEK293 cells and the indistinguishable pattern of the biased A_{2A}R signaling in the NAc and the hippocampus, as well as the similar enhancement of hippocampal LTP triggered by *optoA$_{2A}$R* and CGS21680 supports that *optoA$_{2A}$R* signaling largely captures the physiological function of the native A_{2A}R. Different from opsin-based optogenetics, *opto-A$_{2A}$R* signals through GPCR signaling allows a control of intracellular A_{2A}R signaling by light, which we now report to involve a rapid induction, consistent with similar rapid physiological response ($T_{on1/2} = \sim 1$ s) of other GPCR light-activated chimera. Thus, the temporal and spatial control of specific A_{2A}R signaling afforded by *optoA$_{2A}$R* in freely behaving animals paves the way to probe the role of A_{2A}R in defined forebrain circuits responsible for behaviors ranging from motor control, fear, addiction, mood or decision making.[59–61]

CONFLICT OF INTEREST

The authors declare no conflict of interest.

ACKNOWLEDGMENTS

This work was supported by NIH (NS041083-11, NS073947), the MacDonald Foundation for Huntington's Research, Defense Advanced Research Projects Agency (Grant W911NF-10-1-0059) and Brain and Behavior Research Foundation (NARSAD Independent Investigator Grant). This study was also sponsored by the National Basic Research Program of China (973 Project, 2011CB504602), the Start-up Fund from Wenzhou Medical University (No. 89211010 and No. 89212012), the Zhejiang Provincial Special Funds (No. 604161241), the Special Fund for Building Key National Clinical Resource (Key Laboratory of Vision Science, Ministry of Health, No. 601041241), the Central Government Special Fund for Local Universities' Development (No. 474091314) and by special BUSM research fund DTD 4-30-14. We thank João Peça (CNC) for providing the calibrated light source for the slice experiments.

REFERENCES

1 van Boxtel MP, Schmitt JA, Bosma H, Jolles J. The effects of habitual caffeine use on cognitive change: a longitudinal perspective. *Pharmacol Biochem Behav* 2003; **75**: 921–927.
2 Hameleers PA, Van Boxtel MP, Hogervorst E, Riedel WJ, Houx PJ, Buntinx F, *et al.* Habitual caffeine consumption and its relation to memory, attention, planning capacity and psychomotor performance across multiple age groups. *Hum Psychopharmacol* 2000; **15**: 573–581.
3 Lindsay J, Laurin D, Verreault R, Hebert R, Helliwell B, Hill GB, *et al.* Risk factors for Alzheimer's disease: a prospective analysis from the Canadian Study of Health and Aging. *Am J Epidemiol* 2002; **156**: 445–453.
4 van Gelder BM, Buijsse B, Tijhuis M, Kalmijn S, Giampaoli S, Nissinen A, *et al.* Coffee consumption is inversely associated with cognitive decline in elderly European men: the FINE Study. *Eur J Clin Nutr* 2007; **61**: 226–232.
5 Ritchie K, Carriere I, de Mendonca A, Portet F, Dartigues JF, Rouaud O *et al.* The neuroprotective effects of caffeine: a prospective population study (the Three City Study). *Neurology* 2007; **69**: 536–545.
6 Gelber RP, Petrovitch H, Masaki KH, Ross GW, White LR. Coffee intake in midlife and risk of dementia and its neuropathologic correlates. *J Alzheimers Dis* 2011; **23**: 607–615.
7 Eskelinen MH, Ngandu T, Tuomilehto J, Soininen H, Kivipelto M. Midlife coffee and tea drinking and the risk of late-life dementia: a population-based CAIDE study. *J Alzheimers Dis* 2009; **16**: 85–91.
8 Dall'Igna OP, Fett P, Gomes MW, Souza DO, Cunha RA, Lara DR. Caffeine and adenosine A2a receptor antagonists prevent beta-amyloid (25–35)-induced cognitive deficits in mice. *Exp Neurol* 2007; **203**: 241–245.
9 Cunha GM, Canas PM, Melo CS, Hockemeyer J, Muller CE, Oliveira CR, *et al.* Adenosine A_{2A} receptor blockade prevents memory dysfunction caused by beta-amyloid peptides but not by scopolamine or MK-801. *Exp Neurol* 2008; **210**: 776–781.
10 Arendash GW, Schleif W, Rezai-Zadeh K, Jackson EK, Zacharia LC, Cracchiolo JR, *et al.* Caffeine protects Alzheimer's mice against cognitive impairment and reduces brain beta-amyloid production. *Neuroscience* 2006; **142**: 941–952.
11 Espinosa J, Rocha A, Nunes F, Costa MS, Schein V, Kazlauckas V, *et al.* Caffeine consumption prevents memory impairment, neuronal damage, and adenosine A_{2A} receptors upregulation in the hippocampus of a rat model of sporadic dementia. *J Alzheimers Dis* 2013; **34**: 509–518.
12 Cognato GP, Agostinho PM, Hockemeyer J, Muller CE, Souza DO, Cunha RA. Caffeine and an adenosine A_{2A} receptor antagonist prevent memory impairment and synaptotoxicity in adult rats triggered by a convulsive episode in early life. *J Neurochem* 2010; **112**: 453–462.
13 Duarte JM, Agostinho PM, Carvalho RA, Cunha RA. Caffeine consumption prevents diabetes-induced memory impairment and synaptotoxicity in the hippocampus of NONcZNO10/LTJ mice. *PLoS One* 2012; **7**: e21899.
14 Canas PM, Porciuncula LO, Cunha GM, Silva CG, Machado NJ, Oliveira JM, *et al.* Adenosine A_{2A} receptor blockade prevents synaptotoxicity and memory dysfunction caused by beta-amyloid peptides via p38 mitogen-activated protein kinase pathway. *J Neurosci* 2009; **29**: 14741–14751.
15 Prediger RD, Batista LC, Takahashi RN. Caffeine reverses age-related deficits in olfactory discrimination and social recognition memory in rats. Involvement of adenosine A_1 and A_{2A} receptors. *Neurobiol Aging* 2005; **26**: 957–964.
16 Zhou SJ, Zhu ME, Shu D, Du XP, Song XH, Wang XT, *et al.* Preferential enhancement of working memory in mice lacking adenosine A_{2A} receptors. *Brain Res* 2009; **1303**: 74–83.
17 Wei CJ, Singer P, Coelho J, Boison D, Feldon J, Yee BK, *et al.* Selective inactivation of adenosine A_{2A} receptors in striatal neurons enhances working memory and reversal learning. *Learn Mem* 2011; **18**: 459–474.
18 Yu C, Gupta J, Chen JF, Yin HH. Genetic deletion of A_{2A} adenosine receptors in the striatum selectively impairs habit formation. *J Neurosci* 2009; **29**: 15100–15103.
19 Wei CJ, Augusto E, Gomes CA, Singer P, Wang Y, Boison D, *et al.* Regulation of fear responses by striatal and extrastriatal adenosine A_{2A} receptors in forebrain. *Biol Psychiatry* 2013; **75**: 855–863.
20 Kadowaki Horita T, Kobayashi M, Mori A, Jenner P, Kanda T. Effects of the adenosine A_{2A} antagonist istradefylline on cognitive performance in rats with a 6-OHDA lesion in prefrontal cortex. *Psychopharmacology (Berl)* 2013; **230**: 345–352.
21 Cunha RA, Almeida T, Ribeiro JA. Parallel modification of adenosine extracellula r metabolism and modulatory action in the hippocampus of aged rats. *J Neurochem* 2001; **76**: 372–382.
22 Chen JF, Eltzschig HK, Fredholm BB. Adenosine receptors as drug targets—what are the challenges? *Nat Rev Drug Discov* 2013; **12**: 265–286.
23 Cunha RA, Agostinho PM. Chronic caffeine consumption prevents memory disturbance in different animal models of memory decline. *J Alzheimers Dis* 2010; **20**: S95–116.
24 Chen JF, Sonsalla PK, Pedata F, Melani A, Domenici MR, Popoli P, *et al.* Adenosine A_{2A} receptors and brain injury: broad spectrum of neuroprotection, multifaceted actions and 'fine tuning' modulation. *Prog Neurobiol* 2007; **83**: 310–331.
25 Fredholm BB, Chern Y, Franco R, Sitkovsky M. Aspects of the general biology of adenosine A_{2A} signaling. *Prog Neurobiol* 2007; **83**: 263–276.
26 Shen HY, Canas PM, Garcia-Sanz P, Lan JQ, Boison D, Moratalla R, *et al.* Adenosine A_{2A} receptors in striatal glutamatergic terminals and GABAergic neurons oppositely modulate psychostimulant action and DARPP-32 phosphorylation. *PLoS One* 2013; **8**: e80902.
27 Shen HY, Coelho JE, Ohtsuka N, Canas PM, Day YJ, Huang QY, *et al.* A critical role of the adenosine A_{2A} receptor in extrastriatal neurons in modulating psychomotor activity as revealed by opposite phenotypes of striatum and forebrain A_{2A} receptor knock-outs. *J Neurosci* 2008; **28**: 2970–2975.
28 Ciruela F, Casado V, Rodrigues RJ, Lujan R, Burgueno J, Canals M, *et al.* Presynaptic control of striatal glutamatergic neurotransmission by adenosine A_1–A_{2A} receptor heteromers. *J Neurosci* 2006; **26**: 2080–2087.
29 Keuerleber S, Gsandtner I, Freissmuth M. From cradle to twilight: the carboxyl terminus directs the fate of the A_{2A}-adenosine receptor. *Biochim Biophys Acta* 2011; **1808**: 1350–1357.
30 Mundell S, Kelly E. Adenosine receptor desensitization and trafficking. *Biochim Biophys Acta* 2011; **1808**: 1319–1328.
31 Boyden ES, Zhang F, Bamberg E, Nagel G, Deisseroth K. Millisecond-timescale genetically targeted optical control of neural activity. *Nat Neurosci* 2005; **8**: 1263–1268.
32 Chen JF, Huang Z, Ma J, Zhu J, Moratalla R, Standaert D, *et al.* A(2A) adenosine receptor deficiency attenuates brain injury induced by transient focal ischemia in mice. *J Neurosci* 1999; **19**: 9192–9200.
33 Costenla AR, Diogenes MJ, Canas PM, Rodrigues RJ, Nogueira C, Maroco J, *et al.* Enhanced role of adenosine A(2A) receptors in the modulation of LTP in the rat hippocampus upon ageing. *The European Journal of Neuroscience* 2011; **34**: 12–21.
34 Cognato GP, Agostinho PM, Hockemeyer J, Muller CE, Souza DO, Cunha RA, *et al.* Caffeine and an adenosine A(2A) receptor antagonist prevent memory impairment and synaptotoxicity in adult rats triggered by a convulsive episode in early life. *Journal of Neurochemistry* 2010; **112**: 453–462.
35 Rebola N, Canas PM, Oliveira CR, Cunha RA. Different synaptic and subsynaptic localization of adenosine A2A receptors in the hippocampus and striatum of the rat. *Neuroscience* 2005; **132**: 893–903.
36 Rebola N, Rodrigues RJ, Lopes LV, Richardson PJ, Oliveira CR, Cunha RA. Adenosine A1 and A2A receptors are co-expressed in pyramidal neurons and co-localized in glutamatergic nerve terminals of the rat hippocampus. *Neuroscience* 2005; **133**: 79–83.
37 Rodrigues RJ, Canas PM, Oliveira CR, Cunha RA. Modification of adenosine modulation of acetylcholine release in the hippocampus of aged rats. *Neurobiology of aging* 2008; **29**: 1597–1601.
38 Borroto-Escuela DO, Romero-Fernandez W, Tarakanov AO, Gomez-Soler M, Corrales F, Marcellino D, *et al.* Characterization of the $A_{2A}R$-D_2R interface: focus on the role of the C-terminal tail and the transmembrane helices. *Biochem Biophys Res Commun* 2010; **402**: 801–807.
39 Viosca J, Malleret G, Bourtchouladze R, Benito E, Vronskava S, Kandel ER, *et al.* Chronic enhancement of CREB activity in the hippocampus interferes with the retrieval of spatial information. *Learn Mem* 2009; **16**: 198–209.
40 Britt JP, Benaliouad F, McDevitt RA, Stuber GD, Wise RA, Bonci A. Synaptic and behavioral profile of multiple glutamatergic inputs to the nucleus accumbens. *Neuron* 2012; **76**: 790–803.

41 Chuhma N, Tanaka KF, Hen R, Rayport S. Functional connectome of the striatal medium spiny neuron. *J Neurosci* 2011; **31**: 1183–1192.
42 Kenakin T, Christopoulos A. Signalling bias in new drug discovery: detection, quantification and therapeutic impact. *Nat Rev Drug Discov* 2013; **12**: 205–216.
43 Gerfen CR, Engber TM, Mahan LC, Susel Z, Chase TN, Monsma FJ Jr, *et al.* D_1 and D_2 dopamine receptor-regulated gene expression of striatonigral and striatopallidal neurons. *Science* 1990; **250**: 1429–1432.
44 Hauber W, Munkle M. Motor depressant effects mediated by dopamine D_2 and adenosine A_{2A} receptors in the nucleus accumbens and the caudate–putamen. *Eur J Pharmacol* 1997; **323**: 127–131.
45 Barraco RA, Martens KA, Parizon M, Normile HJ. Role of adenosine A_{2a} receptors in the nucleus accumbens. *Prog Neuropsychopharmacol Biol Psychiatry* 1994; **18**: 545–553.
46 Svenningsson P, Le Moine C, Fisone G, Fredholm BB. Distribution, biochemistry and function of striatal adenosine A_{2A} receptors. *Prog Neurobiol* 1999; **59**: 355–396.
47 Canas PM, Duarte JM, Rodrigues RJ, Kofalvi A, Cunha RA. Modification upon aging of the density of presynaptic modulation systems in the hippocampus. *Neurobiol Aging* 2009; **30**: 1877–1884.
48 Albasanz JL, Perez S, Barrachina M, Ferrer I, Martín M. Up-regulation of adenosine receptors in the frontal cortex in Alzheimer's disease. *Brain Pathol* 2008; **18**: 211–219.
49 Benito E, Barco A. CREB's control of intrinsic and synaptic plasticity: implications for CREB-dependent memory models. *Trends Neurosci* 2010; **33**: 230–240.
50 Bockaert J, Perroy J, Bécamel C, Marin P, Fagni L. GPCR interacting proteins (GIPs) in the nervous system: roles in physiology and pathologies. *Annu Rev Pharmacol Toxicol* 2010; **50**: 89–109.
51 Gsandtner I, Charalambous C, Stefan E, Ogris E, Freissmuth M, Zezula J. Heterotrimeric G protein-independent signaling of a G protein-coupled receptor. Direct binding of ARNO/cytohesin-2 to the carboxyl terminus of the A_{2A} adenosine receptor is necessary for sustained activation of the ERK/MAP kinase pathway. *J Biol Chem* 2005; **280**: 31898–31905.
52 Rajagopal R, Chen ZY, Lee FS, Chao MV. Transactivation of Trk neurotrophin receptors by G-protein-coupled receptor ligands occurs on intracellular membranes. *J Neurosci* 2004; **24**: 6650–6658.
53 Flajolet M, Wang Z, Futter M, Shen W, Nuangchamnong N, Bendor J, *et al.* FGF acts as a co-transmitter through adenosine A_{2A} receptor to regulate synaptic plasticity. *Nat Neurosci* 2008; **11**: 1402–1409.
54 Sun CN, Cheng HC, Chou JL, Lee SY, Lin YW, Lai HL, *et al.* Rescue of p53 blockage by the A_{2A} adenosine receptor via a novel interacting protein, translin-associated protein X. *Mol Pharmacol* 2006; **70**: 454–466.
55 Sun CN, Chuang HC, Wang JY, Chen SY, Cheng YY, Lee CF, *et al.* The A_{2A} adenosine receptor rescues neuritogenesis impaired by p53 blockage via KIF2A, a kinesin family member. *Dev Neurobiol* 2010; **70**: 604–621.
56 Aarts M, Liu Y, Liu L, Besshoh S, Arundine M, Gurd JW, *et al.* Treatment of ischemic brain damage by perturbing NMDA receptor–PSD-95 protein interactions. *Science* 2002; **298**: 846–850.
57 Cook DJ, Teves L, Tymianski M. Treatment of stroke with a PSD-95 inhibitor in the gyrencephalic primate brain. *Nature* 2012; **483**: 213–217.
58 Ji SP, Zhang Y, Van Cleemput J, Jiang W, Liao M, Li L, *et al.* Disruption of PTEN coupling with 5-HT2C receptors suppresses behavioral responses induced by drugs of abuse. *Nat Med* 2006; **12**: 324–329.
59 Wei CJ, Li W, Chen JF. Normal and abnormal functions of adenosine receptors in the central nervous system revealed by genetic knockout studies. *Biochim Biophys Acta* 2011; **1808**: 1358–1379.
60 Gomes CV, Kaster MP, Tome AR, Agostinho PM, Cunha RA. Adenosine receptors and brain diseases: neuroprotection and neurodegeneration. *Biochim Biophys Acta* 2011; **1808**: 1380–1399.
61 Dellu F, Fauchey V, Le Moal M, Simon H. Extension of a new two-trial memory task in the rat: influence of environmental context on recognition processes. *Neurobiol Learn Mem* 1997; **67**: 112–120.